



**FINAL SUMMARY REPORT**  
(Electron Beam Pumped Laser Action in Selenium and  
Tellurium with Applications for Tunable Backward  
Parametric Oscillations)

The Ohio State University

**ElectroScience Laboratory**

(formerly Antenna Laboratory)  
Department of Electrical Engineering  
Columbus, Ohio 43212

**CASE FILE  
COPY**

**FINAL SUMMARY REPORT 2679-2**

15 July 1969

Grant Number NGR 36-008-103

National Aeronautics and Space Administration  
Office of Grants and Research Contracts  
Washington, D.C. 20546

#### NOTICES

When Government drawings, specifications, or other data are used for any purpose other than in connection with a definitely related Government procurement operation, the United States Government thereby incurs no responsibility nor any obligation whatsoever, and the fact that the Government may have formulated, furnished, or in any way supplied the said drawings, specifications, or other data, is not to be regarded by implication or otherwise as in any manner licensing the holder or any other person or corporation, or conveying any rights or permission to manufacture, use, or sell any patented invention that may in any way be related thereto.

The Government has the right to reproduce, use, and distribute this report for governmental purposes in accordance with the contract under which the report was produced. To protect the proprietary interests of the contractor and to avoid jeopardy of its obligations to the Government, the report may not be released for non-governmental use such as might constitute general publication without the express prior consent of The Ohio State University Research Foundation.

FINAL SUMMARY REPORT  
(Electron Beam Pumped Laser Action in Selenium and  
Tellurium with Applications for Tunable Backward  
Parametric Oscillations)

FINAL SUMMARY REPORT 2679-2

15 July 1969

Grant Number NGR 36-008-103

National Aeronautics and Space Administration  
Office of Grants and Research Contracts  
Washington, D.C. 20546

## REPORT

by

THE OHIO STATE UNIVERSITY ELECTROSCIENCE LABORATORY  
(Formerly Antenna Laboratory)  
Columbus, Ohio 43212

**Sponsor** National Aeronautics and Space Administration  
Office of Grants and Research Contracts  
Washington, D.C. 20546

Grant Number NGR 36-008-103

# Investigation of Electron Beam Pumped Laser Action in Selenium and Tellurium with Applications for Tunable Backward Parametric Oscillations

**Subject of Report      Final Summary Report**

Date 15 July 1969

## TABLE OF CONTENTS

	Page
I. INTRODUCTION	1
II. ACCOMPLISHMENTS TO DATE	2
III. SOURCE OF RESIDUAL ABSORPTION IN SE SINGLE CRYSTALS	7
A. <u>Magnitude Of Optical Absorption</u>	7
B. <u>Loss Due To Dielectric Scattering</u>	7
C. <u>Loss Associated With Electronic Levels</u>	10
IV. MATERIAL FABRICATION	13
V. CONCLUSIONS	13
REFERENCES	14

# FINAL SUMMARY REPORT

## I. INTRODUCTION

The peculiar spiral chain structure of trigonal Te, Se, and HgS make these materials of special interest in the investigation of nonlinear optical phenomena. Since no known source (other than nature) produces cinnabar, we will restrict attention to the elemental crystals. The pertinent optical properties of these materials are given in Table I. The large birefringence<sup>1,2</sup> and nonlinear susceptibility<sup>3</sup> suggest a variety of phase matched parametric interactions such as efficient second harmonic generation, up conversion, down conversion, and backward wave oscillation. The narrower transparency range of Te indicates that Se may be of more interest in certain applications requiring high intensity pumping such as can be obtained from a ruby (0.694  $\mu\text{m}$ ) or Nd glass (1.06  $\mu\text{m}$ ) laser. Either material could be pumped with the CO<sub>2</sub> (10.6  $\mu\text{m}$ ) laser.

TABLE I  
OPTICAL PROPERTIES OF Se AND Te

	Se	Te
refractive index (ordinary ray)	2.78	4.8
refractive index (extraordinary ray)	3.48	6.24
nonlinear susceptibility ( $d_{\parallel}$ esu)	$1.9 \times 10^{-7}$ or $5 \times 10^{-7}$	$1.27 \times 10^{-5}$
interband absorption edge (short wave limit)	$0.77 \mu$ (300°K) $0.68 \mu$ (77°K)	$3.8 \mu$
lattice absorption edge (long wave limit)	$20 \mu$	$30 \mu$

Only recently has it been possible to grow large single crystals of Se. This is done by halogen<sup>4</sup> or thallium<sup>5</sup> doping of the melt. The impurity seems to break the ring and chain structure of the polymers in

the melt and thus accelerate the crystallization kinetics. Large ( $\sim$  cm<sup>3</sup>) dimension) single crystals can now be grown for physical investigations and potential device evaluation.

### II. ACCOMPLISHMENTS TO DATE

In Fig. 1 we show our apparatus for Czochralski growth of Se crystals. It had been redesigned from that of the first successful status report by changing to a split-tube furnace, which allows growth at such a low temperature, about 117°C. It is necessary to use a properly insulated furnace in a high-gain temperature control loop. The fiber insulation gives a satisfactory short thermal time constant when the melt temperature rises above the set point.

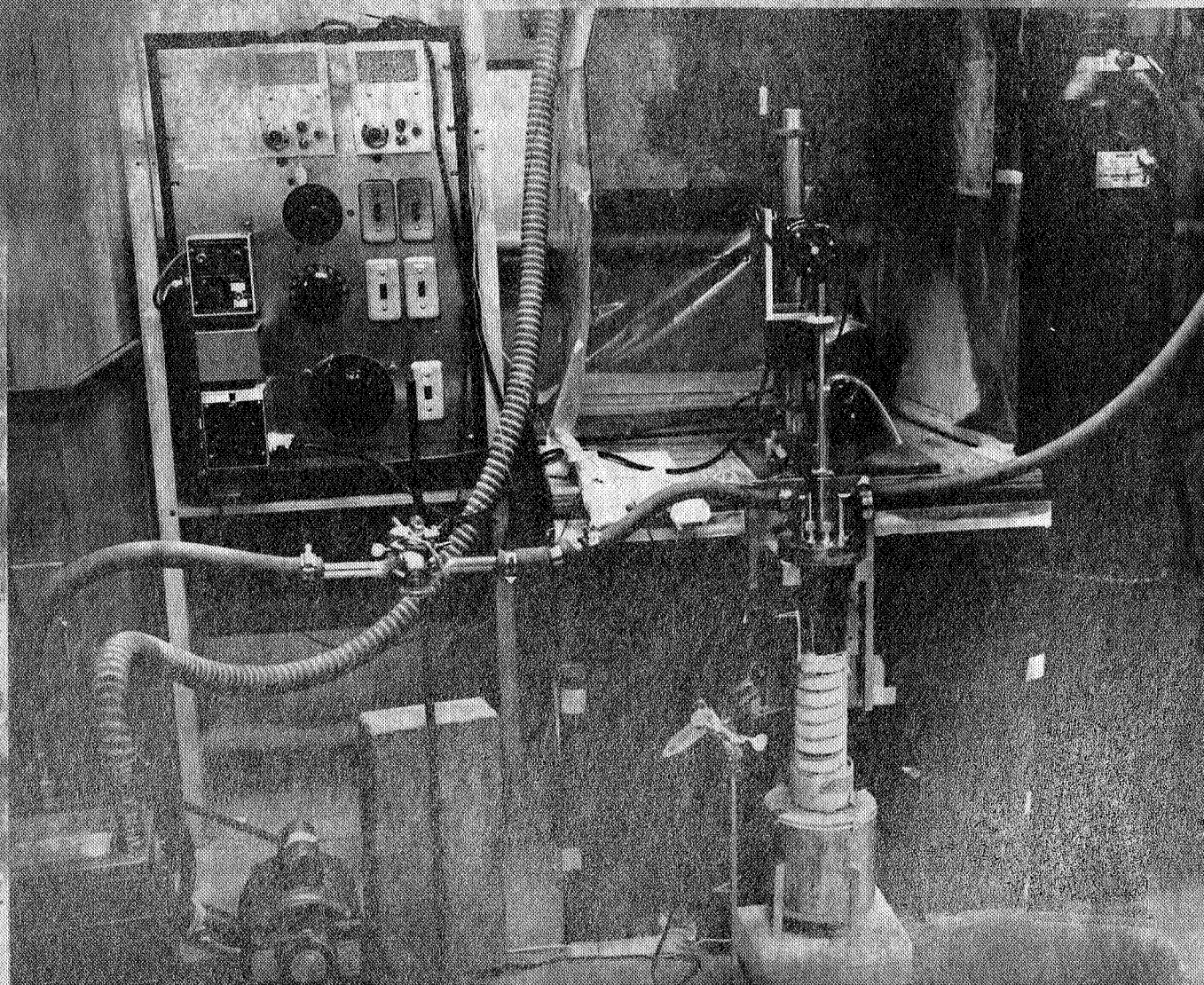


Fig. 1. Redesigned furnace for Czochralski growth of trigonal selenium.

During the year, seven Czochralski growth runs were initiated with the apparatus of Fig. 1. Despite many tries with each seed, only the third run yielded a good sized single crystal. Temperature instability of the melt-crystal interface has been the main problem. This has now been traced to the tape and radiant heaters just above the pot furnace in Fig. 1 and corrective measures are being taken. Many pulls produced what appeared to be a single crystal for the first several millimeters from the seed end before turning polycrystalline, apparently due to a temperature change.

Figure 2 shows one of the best crystals we have pulled. Note the well developed  $[10\bar{1}0]$  faces in the regions  $3/4"$  to  $1\frac{3}{8}"$  and  $3\frac{1}{8}"$  to  $3\frac{3}{4}"$ . These regions were single crystal through the entire ingot. Transmission measurements near the absorption edge at room temperature for this crystal are shown in Fig. 3. The measurement was made with unpolarized light and  $\alpha$  calculated from:

$$\frac{I}{I_0} = 0.5 e^{-\alpha d}$$

where the factor of 0.5 corrects for reflection loss. If appreciable dichroism exists, the measured  $\alpha$  will be that corresponding to the polarization with least loss and  $\alpha_{\parallel}$  and  $\alpha_{\perp}$  will be slightly less than shown in Fig. 3. However, contradictory results on the dichroism of Se have been published<sup>2,7</sup> so we will have to make our own measurements. A spot check of the absorption constant at  $10.6 \mu\text{m}$  gave  $\alpha = 7.9 \text{ cm}^{-1}$  which is not significantly different from the short wavelength value.

To the best of our knowledge, these are the most transparent Czochralski grown crystals to date. Crystal quality seems to be related to restricting the transverse dimensions of the crystal to  $\sim 1/4"$  maximum diameter. However, the modified Bridgeman or traveling solvent technique<sup>5</sup> has been reported to give crystals of superior optical quality.<sup>8</sup> Therefore, the apparatus shown in Fig. 4 was constructed. The desired temperature profile is determined, in part, by the insulation thickness, heater winding density, and heat sink. Each half of the winding, above and below the heat sink, is separately temperature controlled. The heat sink on the Bridgeman apparatus has been water cooled to give a temperature gradient of  $70^\circ\text{C/cm}$ . The profile is shown in Fig. 5, along with a future modification to eliminate the temperature peak. The annealing section of the profile will be reintroduced later.

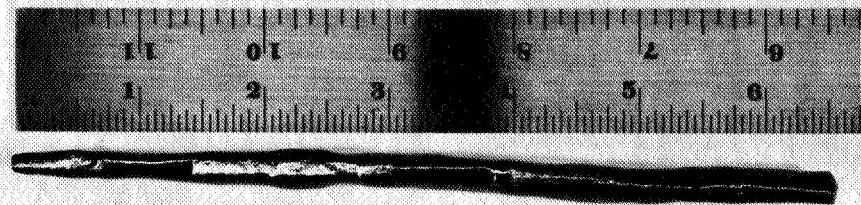


Fig. 2. Czochralski grown Se crystal.

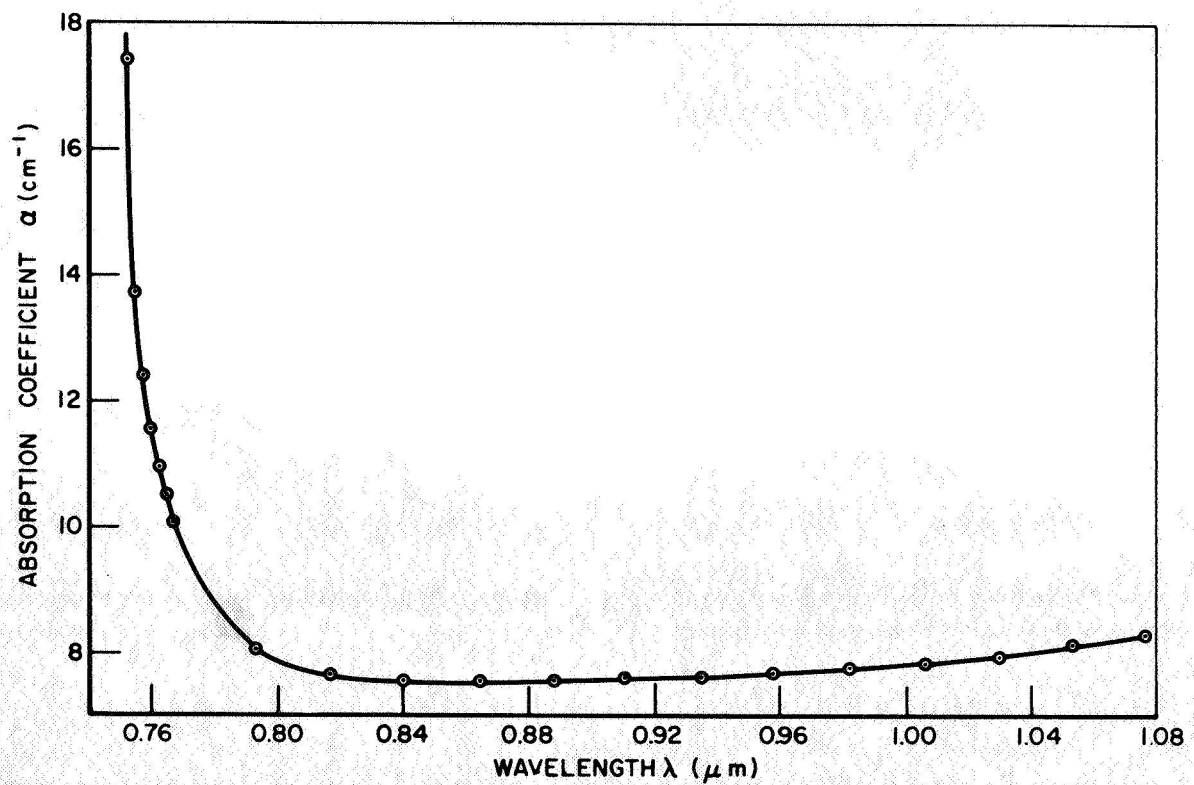


Fig. 3. Absorption coefficient of Se crystal at room temperature.

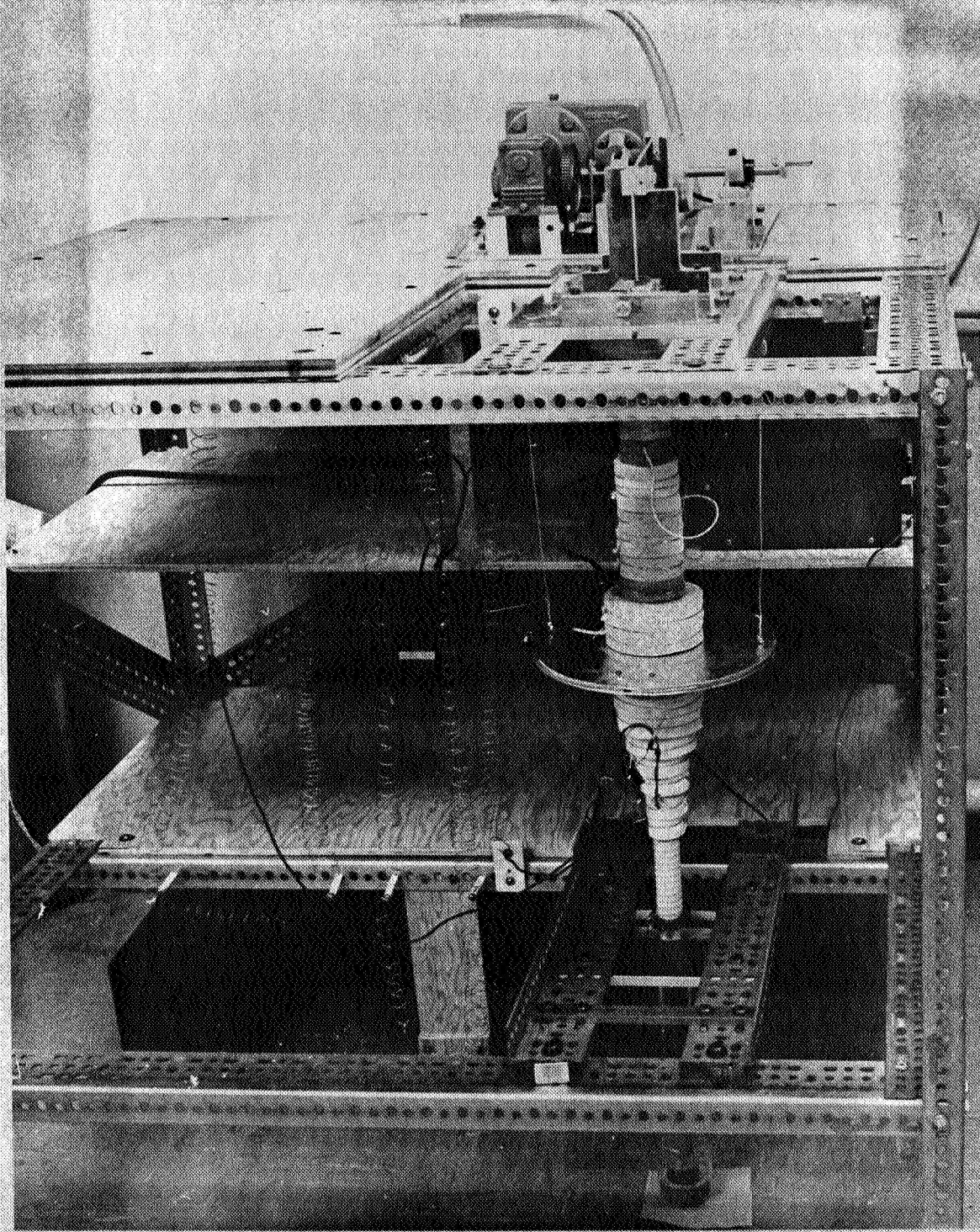


Fig. 4. Modified Bridgeman or traveling solvent  
Se crystal growing apparatus.

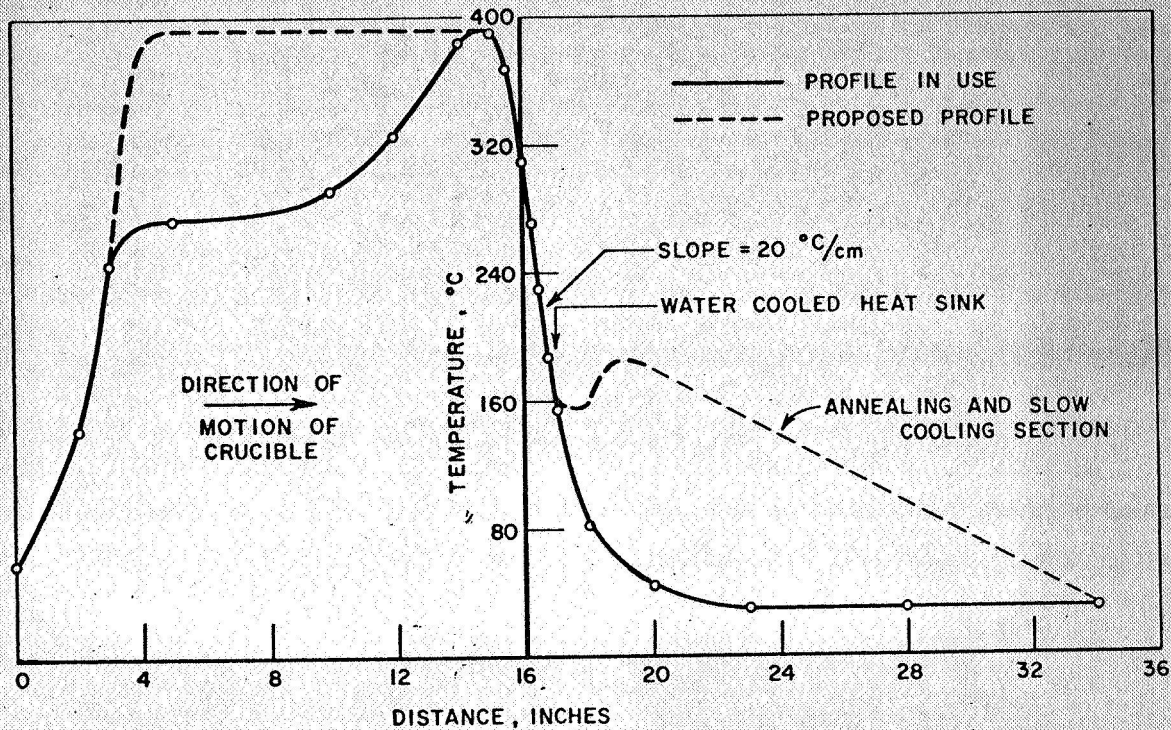


Fig. 5. Temperature profiles of Bridgeman furnace.

Nine crystals have been grown with the Bridgeman technique to date, two with a modified Czochralski apparatus and the others with the apparatus in Fig. 4. [After encouraging results with the first two crystals the quality declined at first with the new apparatus. With succeeding modifications of the Bridgeman apparatus, however, the quality has increased.] Crystal number seven had an absorption coefficient of  $26 \text{ cm}^{-1}$ , which is as transparent as many of the Czochralski crystals and about one third as transparent as the best of them.

The crystals generally start out very polycrystalline and improve as growth progresses. This is thought to be caused in part by divitrification in the quartz crucible due to fabrication techniques. A change in design is pending.

A zone refiner which can be used to purify selenium or grow crystals by a multiple-pass traveling solvent technique has been constructed but has not been put into operation as yet. It will be able to grow 5 crystals at once at varying speeds from seeded or unseeded charges.

### III. SOURCE OF RESIDUAL ABSORPTION IN SE SINGLE CRYSTALS

To produce optical quality single crystals of Se, it is necessary to understand the nature of imperfections in present crystals. A transmission photograph of an early crystal, Fig. 6, shows the strong optical inhomogeneity and absorption along clusters of lines parallel to the c-axis. (The crystal cracked along the center line which is parallel to the c-axis. Also, lines transverse to the crack are polishing scratches in the surface.) This suggests that the optical attenuation may be due to linear defects (i.e., defects of macroscopic dimensions in the longitudinal direction and atomic or microscopic dimensions in the transverse direction.)

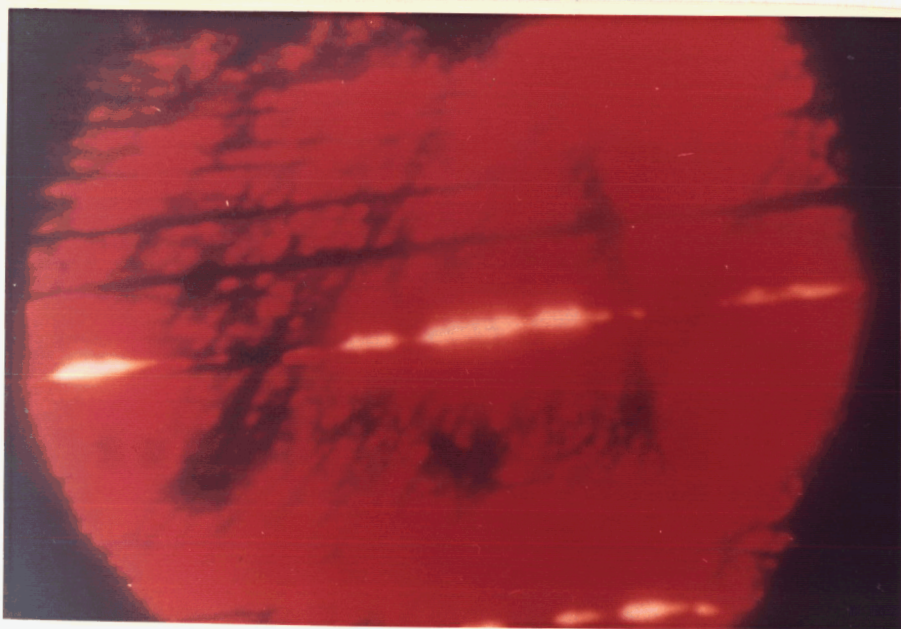
In the following we will outline possible sources of this optical loss and techniques for analysis. We assume that there should be negligible absorption in the region between the inter-band absorption edge and the highest phonon frequency or overtone thereof. Such is indeed the case for the isomorphous crystal, Te, where absorption coefficients of  $10^{-2}$   $\text{cm}^{-1}$  have been measured.<sup>9</sup> Free carrier absorption can be neglected since, for Se over a wide temperature range,  $\rho \sim 10^{14} \text{ cm}^{-3}$ .<sup>10</sup>

#### A. Magnitude Of Optical Absorption

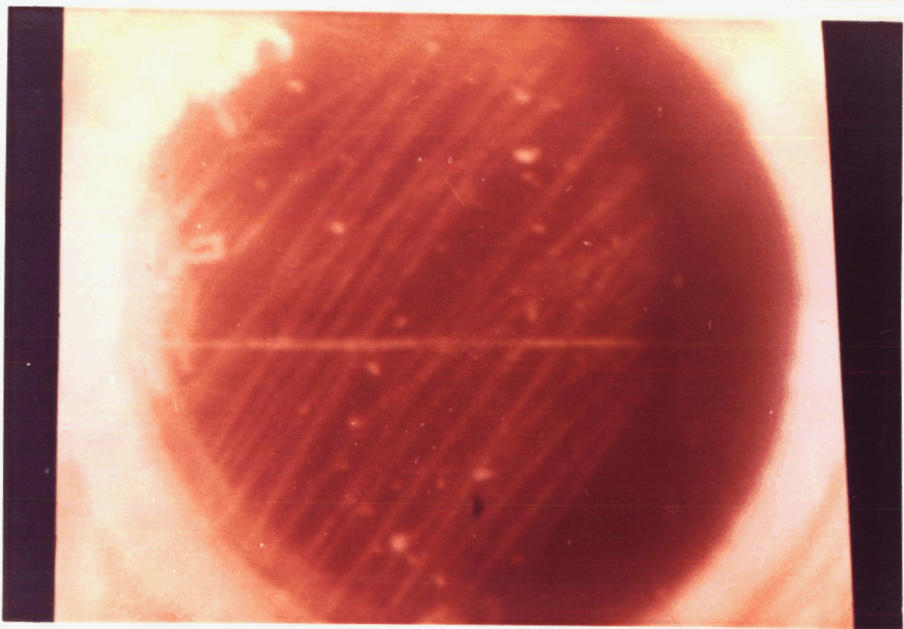
The large absorption in the transparent region of Se is believed due to residual lattice defects. This absorption has gradually decreased over the past decade as better crystals have become available. In 1961, Gobrecht and Tausend reported  $\alpha_{\parallel} = 30 \text{ cm}^{-1}$  and  $\alpha_{\perp} = 20 \text{ cm}^{-1}$  for  $\lambda < 2\mu\text{m}$ .<sup>2</sup> In 1967, Jerphagnon, Batifol, and Sourbe experimented with crystals having  $\alpha(10.6\mu) = 5 \text{ cm}^{-1}$  and  $\alpha(5.3\mu) = 30 \text{ cm}^{-1}$  but unspecified polarization.<sup>11</sup> The best crystals reported to date are by Roberts, Titihasi and Keezer in 1968 with  $\alpha_{\perp} = 7 \text{ cm}^{-1}$  and  $\alpha_{\parallel} = 2 \text{ cm}^{-1}$ .<sup>7</sup> Our best crystals are characterized by  $\alpha \approx 8 \text{ cm}^{-1}$  from  $0.8\mu\text{m}$  to  $1\mu\text{m}$  and at  $10.6\mu\text{m}$ . The short wavelength absorption characteristic is shown in Fig. 3 for a good Czochralski grown crystal.

#### B. Loss Due To Dielectric Scattering

Dichroism in the "transparent" spectral region is remarkable. It is not certain whether this is a true absorption of energy or a scattering from crystal imperfections. Since the most prominent crystal defect is lineage and/or dislocations parallel to the c-axis, we calculated the scattering of electromagnetic waves with electric



(a) Transmission through Se crystal showing effects of crystalline defects.



(b) Surface of Se crystal showing surface scratches, some of which may contribute to loss shown in (a) above.

field vectors polarized parallel and perpendicular to the axis of dielectric cylinders. Lineage would appear as a dielectric cylinder of lower dielectric constant than the bulk crystal while dislocations could be regions of either enhanced or reduced dielectric constant.

For an incident electric field polarized parallel to the c-axis (z direction) and propagating in the x direction

$$\vec{E}_i = \hat{a}_x E_{110} e^{i(k_{\parallel} x - \omega t)}$$

the scattered electric field is given by

$$\vec{E}_s = \hat{a}_z E_{110} \frac{\pi}{4} (k_{\parallel} a)^2 \left(1 - \frac{\epsilon_i}{\epsilon_{\parallel}}\right) H_0^{(1)}(k_{\parallel} r) e^{-i(\omega t + \frac{\pi}{2})}$$

which is valid for  $(k_{\parallel} a) \ll 1$ , where:

$\epsilon_i$  ≡ dielectric constant of cylinder

$\epsilon_{\parallel}$  ≡ dielectric constant of Se with  $\vec{E}$  parallel to c-axis

$a$  ≡ radius of scattering cylinder

$k_{\parallel}$  ≡  $2\pi\sqrt{\epsilon_{\parallel}}/\lambda$

$H_m^{(1)}(k_{\parallel} r)$  ≡ Hankel function of first kind.

This results in an attenuation coefficient given by

$$\alpha_{\parallel} = \frac{\pi^2}{4} (k_{\parallel} a)^3 \left(1 - \frac{\epsilon_i}{\epsilon_{\parallel}}\right)^2 a N_s \text{ cm}^{-1}$$

where  $N_s$  is the number of scattering centers per unit area ( $\text{cm}^{-2}$ ).

For an incident electric field polarized perpendicular to the c-axis, it is more convenient to work with the corresponding incident magnetic field:

$$\vec{H}_i = \hat{a}_z H_{110} e^{i(k_{\perp} x - \omega t)}$$

which gives a scattered magnetic field of

$$\vec{H}_s = \hat{a}_z H_{110} \frac{\pi}{2} (k_{\perp} a)^2 \frac{\left(1 - \frac{\epsilon_i}{\epsilon_{\perp}}\right)}{\left(1 + \frac{\epsilon_i}{\epsilon_{\perp}}\right)} \cos \theta H_1^{(1)}(k_{\perp} r) e^{-i\omega t}$$

where

$\epsilon_{\perp}$   $\equiv$  dielectric constant of Se with E perpendicular to c-axis

$$k_{\perp} \equiv 2\pi\sqrt{\epsilon_{\perp}}/\lambda$$

The resultant attenuation is given by

$$\alpha_{\perp} = \frac{\pi^2}{2} (k_{\perp} a)^3 \left( \frac{1 - \frac{\epsilon_i}{\epsilon_{\perp}}}{1 + \frac{\epsilon_i}{\epsilon_{\perp}}} \right)^2 \text{ a N}_s \text{ cm}^{-1}$$

The expressions for  $\alpha_{\perp}$  and  $\alpha_{\parallel}$  indicate that this is probably not the mechanism of attenuation since  $\alpha_{\perp}$  and  $\alpha_{\parallel}$  both predict an inverse cube dependence on wavelength which is not observed.<sup>2</sup>

### C. Loss Associated With Electronic Levels

We must therefore look for electronic transitions due to defect levels introduced by crystal imperfections as the source of this residual absorption. Since Se is a semiconductor with a band gap of  $\sim 1.6$  eV (or  $\sim 1.8$  eV for  $T \gtrsim 77^{\circ}\text{K}$ ), the methods of semiconductor physics may be useful in determining the nature of the optically active centers. Optical absorption will be to centers located in the forbidden band of the "perfect" crystal.

The energy of impurity or defect levels in high resistivity semiconductors may be determined by the method of thermally stimulated currents.<sup>12</sup> A distribution of levels 0.065 eV to 0.3 eV deep has been reported.<sup>13</sup> The deeper levels appear in crystals which have undergone large plastic deformation. In Fig. 7 a complete thermally stimulated current curve is presented for an Se sample cleaved from a Bridgeman grown crystal. The peak at  $T^* = 114^{\circ}\text{K}$  is associated with a discrete level at 0.2 eV above the valence band edge. The broad maximum from  $130^{\circ}\text{K}$  to  $220^{\circ}\text{K}$  is associated with a distribution of shallow levels. These

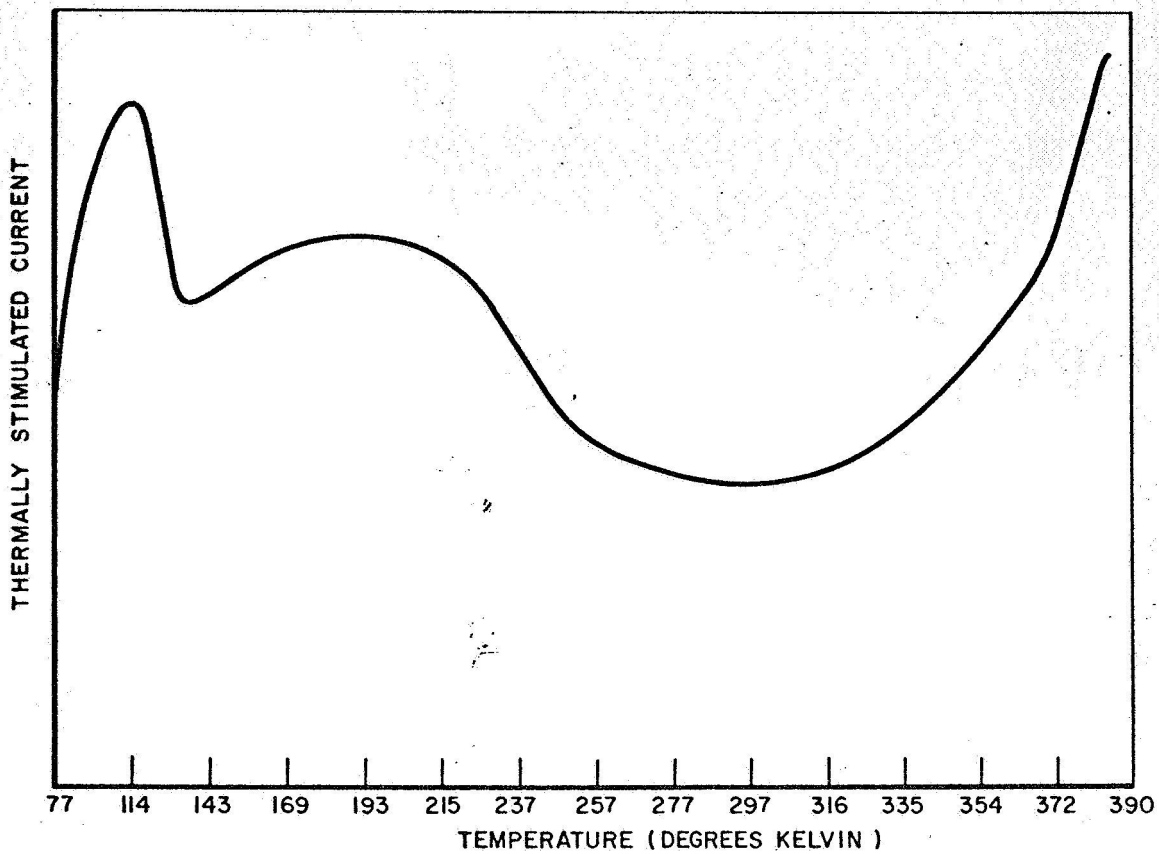


Fig. 7. Trace of complete thermally stimulated current run showing peaks due to a discreet level and a distribution of levels.

are analysed by a series of "trap cleaning" runs<sup>12</sup> wherein the temperature rise is halted in the middle of a run and the crystal recycled to a low temperature and the thermally stimulated current run retraced. The data, replotted in Fig. 8 as  $\log I$  vs  $1/T$ , shows a distribution of very shallow levels from 0.0445 eV to 0.0324 eV deep. This is in accord with the better transparency of Bridgeman grown crystals. The source of the 0.2 eV level is as yet unknown. It may be due to the Tl introduced in the crystal to accelerate growth. Optical properties of the Tl impurity have not yet been investigated.

For satisfactory identification of defect levels, optical, electrical, crystallographic, and chemical techniques will have to be employed on individual crystals.

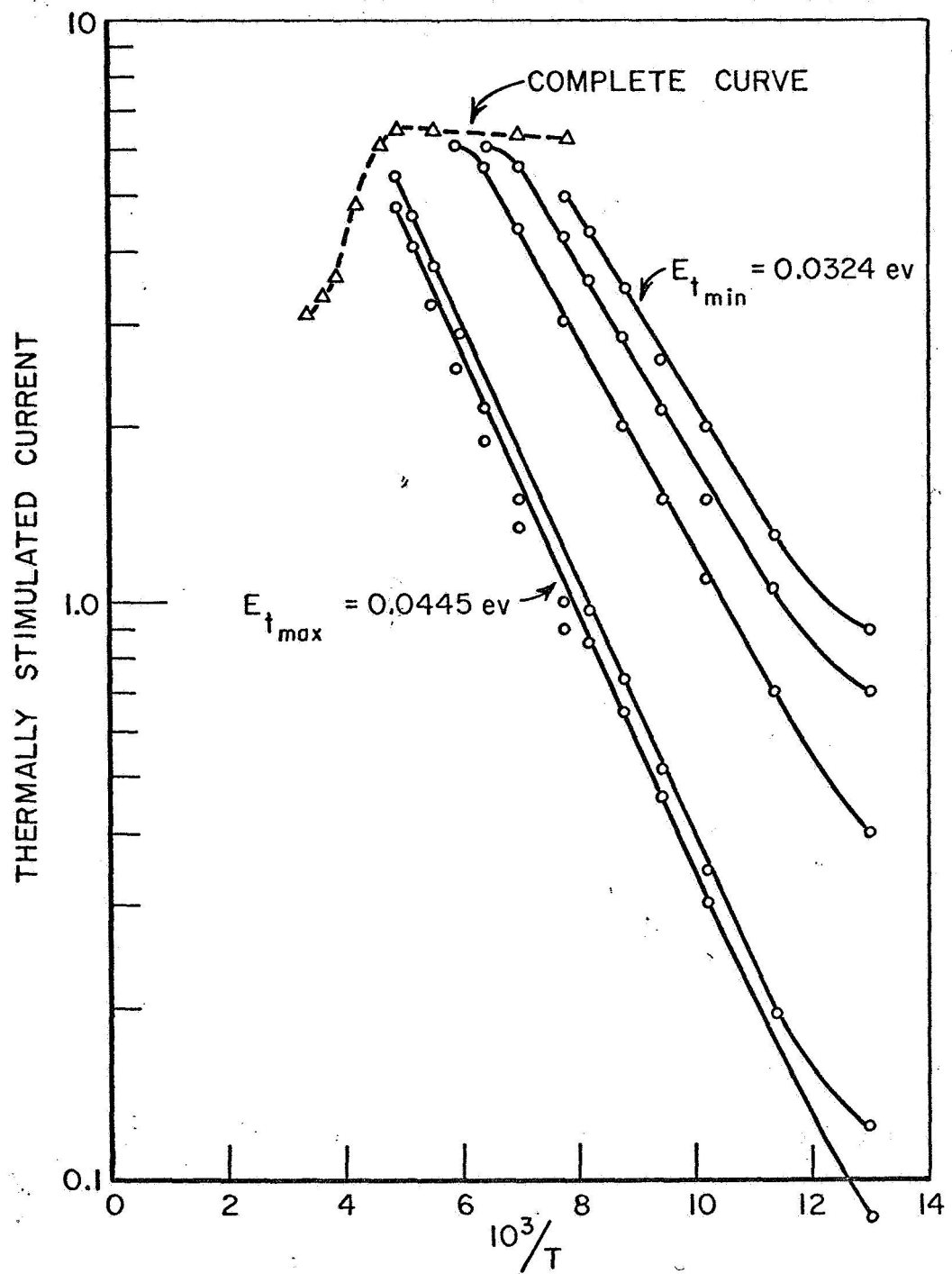


Fig. 8. Thermally stimulated current from a series of "trap cleaning" runs plotted against  $1/T$  to determine activation energies of the traps.

#### IV. MATERIAL FABRICATION

Single crystal Se is exceedingly fragile due to the weak Van der Waals bonds between chains. Cutting, lapping, polishing, cleaning or even careful handling can introduce surface or bulk damage. Se is weaker than Te<sup>14</sup> which, in turn, is notorious. Cotton will scratch the crystal surface and handling with tweezers introduces dislocations.

To cut the material, we slide the crystal into a loose fitting glass tube and fill with a low melting point wax (glycol phthalate). The ensemble is then sliced with a wire saw and abrasive slurry. The glass carries the full weight of the wire saw. As the glass is cut, the Se is also cut, but without having any pressure applied to force the wire through the soft crystal. Without removing the crystal from the encapsulation, the surface is etched to remove surface damage from the sawing operation. For room temperature experiments, it is best to leave the crystal in the encapsulating disk to avoid damage due to handling. Any encapsulating compound could probably be used which does not contract or dilate upon setting.

#### V. CONCLUSION

Single crystals of trigonal Se have been grown of adequate size for nonlinear optical experiments. However, the absorption is still too high for many purposes. With additional work, mainly in the area of improved temperature control, the absorption coefficient should be brought down to  $1 \text{ cm}^{-1}$ . It may be possible to do better than this but there is, at present, no sure evidence that it can be done. Te and mixed crystals of  $\text{Te}_x \text{S}_{1-x}$  on the Te rich side should have the lower attenuation characteristic of Te.

## REFERENCES

1. R.S. Caldwell and H.Y. Fan, Phys. Rev. 114, 664 (1959).
2. H. Gobrecht and A. Tausend, Z. fur Physik 161, 205 (1961).
3. C.K.N. Patel, Phys. Rev. Letters, 16, 613 (1966).
4. R.C. Keezer and J.W. Moody, Applied Phys. Letters 8, 233 (1966).
5. R.C. Keezer, C. Wood, and J.W. Moody, J. Phys. Chem. Solids Suppl. 1, 119 (1967).
6. The Ohio State University ElectroScience Laboratory Semiannual Statue Report 2679-1, (1969).
7. G.G. Roberts, S. Titihasi, and R.C. Keezer, Phys. Rev. 166, 637 (1968).
8. R.C. Keezer, private communication.
9. J.S. Blakemore and K.C. Nomura, Phys. Rev. 127, 1024 (1962).
10. K. Plesoner, Proc. Phys. Soc. B 64, 671 (1951).
11. J. Jerphagnon, B. Batifol and M. Sourbe, Comptes Rendus, Series B 265, 400 (1967).
12. K.H. Nicholas and J. Woods, Brit. J. Appl. Phys. 15, 783 (1964).
13. J. Stuke, Phys. Stat. Sol. 6, 441 (1964).
14. J. Mort, J. Appl. Phys. 38, 3414 (1967).
15. H.J. Queisser and J. Stuke, 5, 75 (1967).
16. W.W. Anderson, Phys. Rev. 136, A556 (1964).